

## Inverse-fluorescence correlation spectroscopy: more information and less labeling

Stefan Wennmalm, Jerker Widengren

Department of Applied Physics, Experimental Biomolecular Physics, Royal Institute of Technology, SE-106 91 Stockholm, Sweden

### TABLE OF CONTENTS

1. Abstract
2. Introduction
3. Theory
  - 3.1. iFCS
  - 3.2. iFCCS
4. Applications
  - 4.1. Label-free estimation of the size and concentration of particles/biomolecules using iFCS
  - 4.2. Direct estimation of the volume of particles/biomolecules using iFCCS
  - 4.3. Analysis of interactions between labeled ligands and unlabeled particles/biomolecules using iFCCS
5. General considerations and discussion
6. Perspective
7. Acknowledgements
8. References
  
9. Keywords
10. Corresponding author

## 1. ABSTRACT

Inverse-Fluorescence Correlation Spectroscopy (iFCS) is a recently developed modification of standard FCS that allows analysis of particles and biomolecules without labeling. The particles generate no signal; instead the signal is generated by a surrounding medium. Particles diffusing through the FCS-detection volume displace a fraction of the surrounding medium, causing transient dips in the detected signal. These give information about the mobility and concentration of the analyzed particles. Also labeled particles can be analyzed, whereby their signal is cross-correlated with that from the surrounding medium (iFCCS). This can give information about the volume of the labeled particles, or alternatively about the size of the detection volume. Also the interaction of unlabeled particles with small, labeled ligands can be analyzed with iFCCS. This allows using cross-correlation as a sensitive indication of binding, even though only one binding-partner is labeled. This review describes the principles of iFCS and iFCCS and measurements of microspheres dissolved in a surrounding medium containing alexa 488. We also discuss practical considerations, and future possibilities for analyses of biomolecules.

## 2. INTRODUCTION

The theory and first experiments of standard Fluorescence Correlation Spectroscopy (FCS) were introduced in 1972 by Magde, Elson and Webb (1,2). They studied fluorescence bursts from dye-labeled biomolecules diffusing through an open detection volume. By autocorrelation of the fluorescence signal, information can be obtained about concentrations (nM) and molecular sizes, and in principle about any dynamic process that yields fluctuations between states of different fluorescence brightness. The use of FCS has increased tremendously since 1993, when a significantly improved signal to noise ratio was accomplished (3). FCS and related methods have since then become important tools in biophysics and cell biology, in academia as well as in industry (4-8). Commercial, easy-to-use FCS-instruments are today manufactured and sold by most of the major microscopy companies. FCS-based methods are also used in high-throughput screening, in the search for small-molecule drug candidates (5).

A requirement in standard FCS is that analyzed biomolecules are labeled. This constitutes a limitation, since attachment of a fluorescent marker to e.g. a protein is

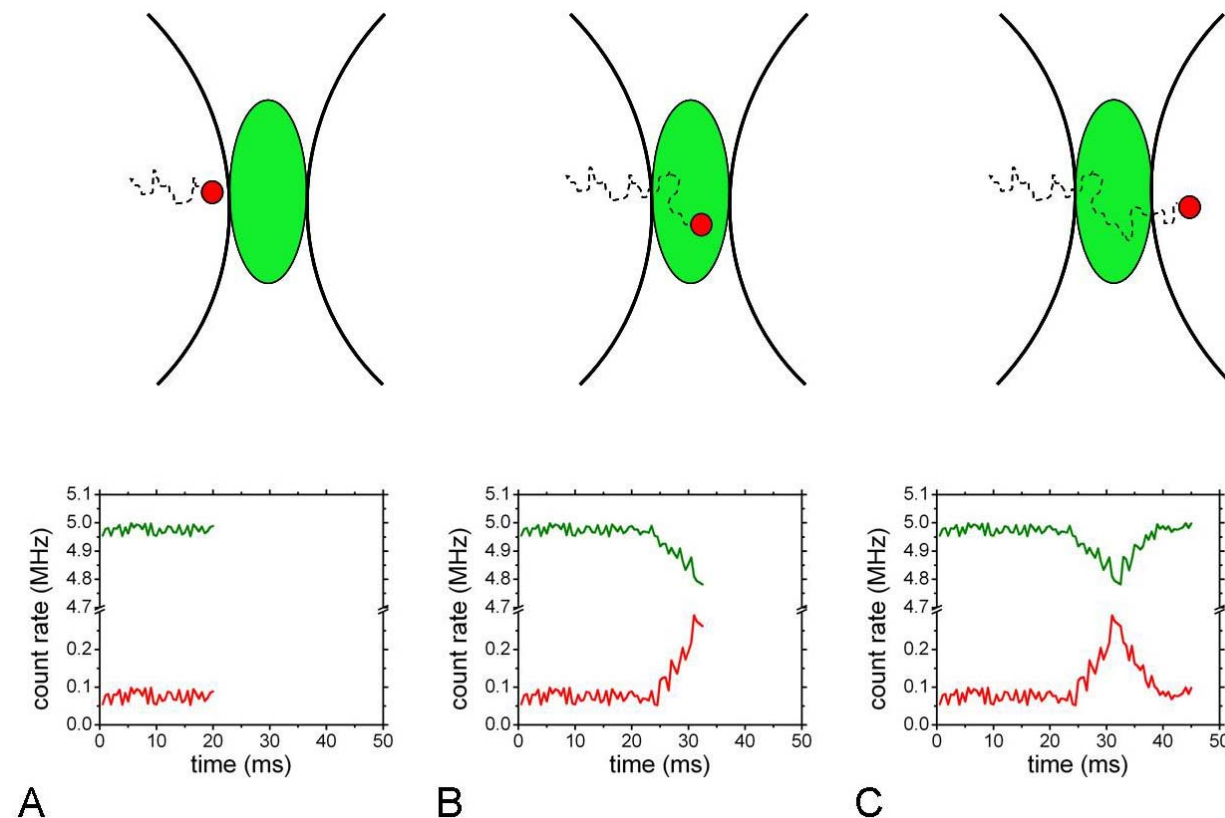


**Figure 1.** Principle of iFCS and iFCCS. A) Fluorescence is detected simultaneously from the particle-channel (red) and the medium-channel (green), and no particle is present in the detection volume. B) A particle has entered the detection volume, resulting in an increased signal in the red channel and a reduced signal in the green channel. C) The particle has left the detection volume, and both signals are restored. Autocorrelation of the signal from the green channel, corresponding to iFCS, gives information about the total concentration of particles, labeled and unlabeled, and about their diffusion coefficient. Autocorrelation of the signal from the red channel (standard FCS), and cross-correlation of the signals from the green and the red channels resulting in anti-correlation (iFCCS), can be calculated simultaneously.

time consuming, sometimes complicated, and may in addition perturb the proteins (9).

iFCS allows the analyzed particles/biomolecules to remain unlabeled, since the signal is generated by the surrounding medium and not by the particles themselves. A particle transiting the FCS-detection volume displaces a fraction of the surrounding medium, causing a dip in the detected signal (Figure 1). As in standard FCS, autocorrelation of the fluctuating signal gives information about the mobility and concentration of the analyzed particles (10) (Figure 2a).

If instead fluorescently labeled particles are analyzed in a surrounding signal-generating medium, cross-correlation of the signals from two spectrally separated detection-channels as in FCCS (11), from labeled particles and from the surrounding medium, results in inverse-Fluorescence Cross-Correlation Spectroscopy (iFCCS, Figure 1 and Figure 2b,c) (12). The amplitude of the iFCCS curve can give information about the ratio between the average size of an analyzed particle and the size of the detection volume. This gives a direct and very sensitive

estimate of the volume of the analyzed particles (Figure 2b). Alternatively, if the size of the analyzed particles is known, the amplitude of the iFCCS-curve yields an estimate of the size of the detection volume. Another possibility using iFCCS is to measure the interaction between small, labeled ligands and larger, unlabeled particles. Cross-correlation in the form of anti-correlation will then appear as the result of binding between ligands and particles, due to dips in the medium-signal coinciding with positive spikes in the ligand-signal. This anti-correlation is a very specific indication of binding, and only one of the binding partners need to be labeled (Figure 2c). Moreover, the fraction of ligand-carrying particles can be determined accurately, since the amount of unlabeled and labeled particles are estimated independently.

### 3. THEORY

#### 3.1. iFCS

Inverse-FCS is closely related to standard FCS, with the same dependence of the autocorrelation and cross-correlation functions on particle mobility. In standard FCS,

## Inverse-FCS: more information and less labeling

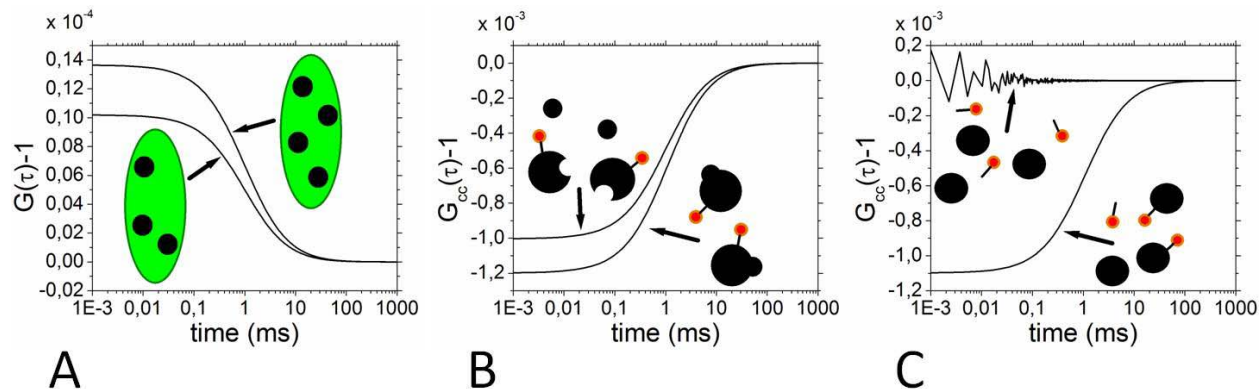


**Figure 2.** Cartoons describing three examples of iFCS- and iFCCS-measurements. A) iFCS-measurement on unlabeled particles at concentrations of  $N$  equal to 3 and  $N$  equal to 4. Because the amplitude of the ACF is proportional to the particle concentration (10), the curve corresponding to  $N$  equal to 4 has 33 percent higher amplitude. B) iFCCS-measurement, anti-correlation, of red-labeled particles which can bind a smaller, unlabeled particle. The surrounding medium would in this example be green, but is not shown. The increase in amplitude of the iFCCS-curve shown corresponds to a 20 percent increase in volume of the labeled particles, a size-increase which is difficult to detect with standard FCS. Given no cross-talk between the detection channels, the amplitudes are for practical purposes independent on particle-concentration, and are only dependent on the volume of the particles (12). C) iFCCS-measurement of unlabeled particles which can bind to small, red-labeled ligands. Again the surrounding medium would be green, but is not shown. Due to their small size, the ligands generate no negative spikes in the medium-signal when transiting the detection volume, and accordingly anti-correlation between the red and the green detection channels will only emerge as a result of binding between the ligands and the larger particles (12). Comparison between the total number of particles and the number of ligand-carrying particles gives a direct estimate of the fraction of ligand-carrying particles.

for the case where translational diffusion of the molecules is the only process generating fluorescence fluctuations, the ACF is given by (13)

$$G(\tau) = \frac{\langle I(t) \cdot I(t+\tau) \rangle}{\langle I(t) \rangle^2} = \frac{1}{\left( \sum_j Q_j N_j \right)^2} \sum_i Q_i^2 N_i \frac{1}{1 + \frac{\tau}{\tau_{Di}}} \frac{1}{\sqrt{1 + \frac{\tau \cdot \omega_0}{\tau_{Di} \cdot z_0}}} \quad (1).$$

Here  $I$  is the detected fluorescence intensity. The model includes  $n$  different diffusion species, with corresponding average numbers  $N_i$  in the detection volume, and characteristic diffusion times  $\tau_{Di}$ .  $\omega_0$  and  $z_0$  denote the distances from the center of the focal plane in the radial and axial dimensions respectively, at which the average detected fluorescence intensity has dropped to  $e^{-2}$  of its peak value.

While the dependence on particle mobility is the same in iFCS as in standard FCS, the dependence on particle concentration is however different. Assuming  $I(t)$  is a stationary process,  $\delta I$  is the deviation from the mean intensity  $\text{mean}I$  at a certain time point, ( $\delta I(t)$  equals  $I(t) - \text{mean}I$ ). From eq. 1 the amplitude, for standard FCS as well as iFCS, follows as

$$G(0) - 1 = \frac{\langle \delta I(0)^2 \rangle}{\langle I \rangle^2} \quad (2).$$

Using that  $V_q$  equals  $V_{\text{part}}/V_{\text{dv}}$  where  $V_{\text{part}}$  is the volume of a particle and  $V_{\text{dv}}$  is the size of the detection volume, that the fluorescence intensity  $I$  equals  $I_{\text{dv}} (1 - N_p V_q)$  where  $I_{\text{dv}}$  is the

total fluorescence intensity from the medium in the detection volume when no particles are present, and that  $N_p$  is the average number of particles in the detection volume, the amplitude in iFCS is given by (10)

$$G(0) - 1 = \frac{(-V_q \cdot I_{\text{dv}} \cdot \sqrt{N_p})^2}{I_{\text{dv}}^2 \cdot (1 - N_p \cdot V_q)^2} = \frac{N_p}{\left( \frac{1}{V_q} - N_p \right)^2} \quad (3).$$

From eq. 3 follows that the amplitude in iFCS is directly proportional to  $N_p$  as long as the denominator  $(1/V_q - N_p)^2$  is approximately constant. As an example, if measurements are performed on microspheres of 100 nm diameter in a detection volume  $V_{\text{dv}}$  of 0.3 fl, then for particle concentrations up to  $N_p$  equal to 3, a doubling of  $N_p$  changes the denominator by less than 1 percent.

Fluctuations in the number of medium-fluorophores in the detection volume will in principle also affect the ACF, however because of their high concentration, usually higher than micro M, the effect on the ACF can be neglected.

Eq. 3 is analogous to the expression for the amplitude in standard FCS for the case of a non-negligible background signal,  $G(\tau) - 1 = \frac{N}{(N + N_B)^2}$  (14), where

$N_B$  is the number of fluorescent molecules equivalent to the background level. The signal from the surrounding medium

## Inverse-FCS: more information and less labeling

in iFCS can be seen as a high background signal, and  $1/V_q$  then corresponds to  $N_B$ .

### 3.2. iFCCS

For standard FCCS as well as iFCCS, the amplitude of the cross-correlation function, for fluorescent molecules predominantly emitting in a green (g) and a red (r) channel respectively, is given by

$$G_{cc}(0) - 1 = \frac{\langle \delta I_g(0) \cdot \delta I_r(0) \rangle}{\langle I_g \rangle \cdot \langle I_r \rangle} \quad (4).$$

By using the full expressions for the fluorescence intensity in the green and the red channels, a general expression for  $G_{cc}(0) - 1$  can be obtained (12). An approximation of the general expression which is more convenient to work with is however

$$G_{cc}(0) - 1 = \frac{-Q_p \cdot N_{pg} \cdot V_{qg} \cdot \sqrt{\frac{V_r}{V_g}}}{I_{ct} + Q_p \cdot N_{pg} \cdot \frac{V_r}{V_g}} \quad (5).$$

Here,  $N_{pg}$  is the average number of particles in the green detection volume,  $V_{qg}$  equals  $V_{part}/V_g$ , where  $V_g$  and  $V_r$  are the sizes of the green and the red detection volumes respectively,  $Q_p$  is the fluorescence intensity per particle (red channel), and  $I_{ct}$  is the intensity in the red channel originating from cross-talk from green fluorescence. Eq. 5 describes the amplitude in iFCCS when labeled particles/biomolecules are analyzed with an error of less than 1 percent, as long as the particles together occupy less than 1 percent of the detection volume (12). For a diffraction-limited detection volume, and for particles of 100 nm diameter this roughly corresponds to  $N_{pg}$  less than 10. For smaller particles or biomolecules it corresponds to even higher numbers. If  $I_{ct}$  equals 0, eq. 5 reduces to

$$G_{cc}(0) - 1 = V_{qg} \cdot \sqrt{\frac{V_g}{V_r}}, \text{ which means that as long as the}$$

approximation is valid,  $G_{cc}(0) - 1$  is independent on the number of particles  $N_{pg}$ . Thus, if  $I_{ct}$  equals 0,  $V_{qg}$  is simple to estimate. However also in the presence of cross-talk it is straightforward to estimate  $V_{qg}$  from eq. 5, by using the measured values of  $Q_p$ ,  $N_{pg}$ , and  $I_{ct}$  (12).

## 4. APPLICATIONS

### 4.1. Label-free estimation of the size and concentration of particles/biomolecules using iFCS

Using a standard FCS-microscope, with a diffraction-limited detection volume and avalanche photodiode (APD) detectors, the concentration and size of particles down to approximately 100 nm diameter can be estimated by iFCS (10). As was discussed in the context of eq. 3 above, the amplitude is directly proportional to

particle concentration under normal measuring concentrations (Figure 3a).

The dependence of the ACF on particle mobility is the same in iFCS as in standard FCS. A difference compared to standard FCS is that the particle size affects not only the decay-time of the ACF, but also the amplitude. For the case when particles of two different sizes are present in the sample, the amplitude is given by

$$G(0) - 1 = \frac{V_{part1}^2 \cdot N_1 + V_{part2}^2 \cdot N_2}{(V_{dv} - V_{part1} \cdot N_1 - V_{part2} \cdot N_2)^2} \quad (6).$$

Here  $V_{part1}$  and  $V_{part2}$  are the volumes of particle types 1 and 2 respectively, and  $N_1$  and  $N_2$  are their corresponding average numbers in the detection volume. Consequently, in eq. 6 the volume of the particles plays the same role in the numerator as the brightness of the particles does in the corresponding expression for standard FCS, where the contribution of a molecular species scales with the square of its brightness (compare with eq. 1). In eq. 6, the particle size has a considerable weight; as an example, if particle 2 has twice the diameter of particle 1, its amplitude will be weighted 64 times that of particle 1. This property makes iFCS very sensitive to size-changes, which could be useful for example for analyzing aggregation processes.

### 4.2. Direct estimation of the volume of particles/biomolecules using iFCCS

If measurements are performed on labeled particles or biomolecules, the positive signal from a transiting labeled particle will coincide with a negative spike in the signal from the medium. Cross-correlation of the two signals will result in anti-correlation (Figure 2b,c and Figure 4), and makes two types of analyses possible: Firstly, when measurements are performed on labeled particles, an estimate of  $V_{qg}$  (equal to  $V_{part}/V_g$ ) can be obtained by use of eq. 5. If the size of the particles size is known,  $V_{qg}$  will give an estimate of  $V_g$  (12). This gives a direct estimate of the size of the detection volume, in contrast to the estimation from standard FCS, where the detection volume is calculated from the  $1/e^2$ -radius omega, which is estimated from measurement on a dye with known diffusion coefficient. An advantage of the iFCCS-approach for estimating the size of the detection volume is that the estimate is independent from viscosity and temperature. If instead the size of the detection volume is estimated prior to measurement,  $V_{qg}$  will give a direct estimate of the volume of the analyzed particles/biomolecules (12). This direct approach has the potential to give a more precise estimate of particle volume than the indirect approach of standard FCS, where the size is estimated via the diffusion coefficient. If the volume of the analyzed particles/proteins in a sample were doubled, due to binding of another particle/protein, the effect in iFCCS would be a doubling of the amplitude (given negligible cross-talk between the detection channels) combined with an increase of the diffusion time  $\tau_D$  of 26 percent, since  $\tau_D$  is proportional to  $(m_2/m_1)^{1/3}$ . However if the analysis were performed

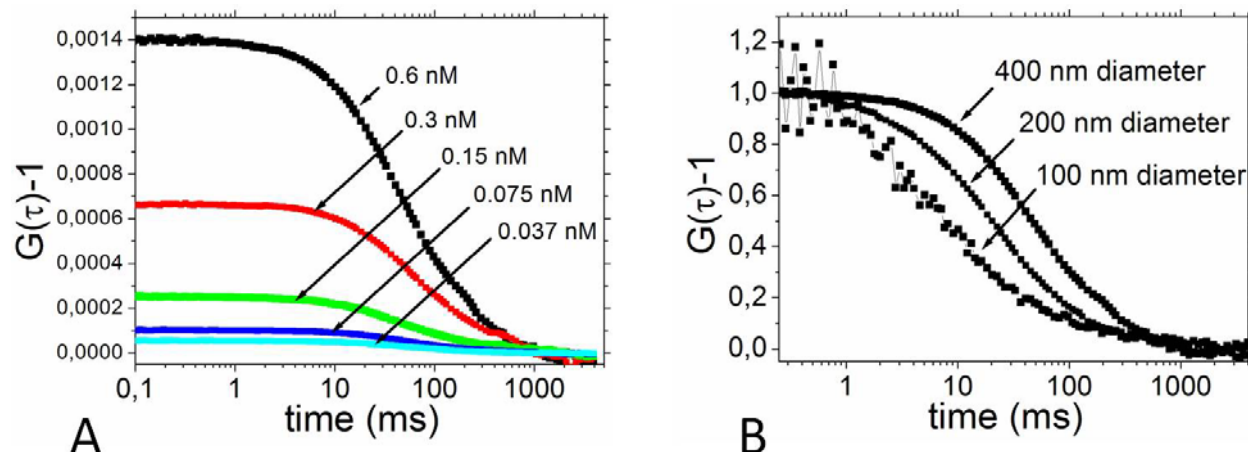


**Figure 3.** A) Experimental autocorrelation curves of unlabeled polystyrene microspheres of 400 nm diameter, measured in 400 micro M alexa 488 dissolved in water, containing 0.5 percent Triton X-100. The amplitude increases approximately linearly with particle concentration (eq. 3). The concentration for the curve with highest amplitude was estimated to 0.6 nM using eq. 3, and the lower concentrations are taken as dilutions by a factor 2 from 0.6 nM. B) Normalized iFCS-curves from measurements on polystyrene microspheres of 100, 200 and 400 nm diameter, with corresponding diffusion times  $\tau_D$  of 7, 20 and 54 ms. As expected for particles that are too large to be considered point-like, the diffusion time increases slightly more than in direct proportion to the particle radius (10, 16, 17).

using standard FCS, only the 26 percent increase of the diffusion time  $\tau_D$  would be observed.

#### 4.3. Analysis of interactions between labeled ligands and unlabeled particles/biomolecules using iFCCS

The second possibility given by iFCCS is to measure the binding of small, dye-labeled ligands to larger, unlabeled particles or biomolecules. When particles and ligands are not bound to each other, the particles will only leave a footprint in the medium-channel (green) and ligands, due to their small size, will only leave a footprint in the dye-label-channel (red). Upon binding however, transiting particles will result in coinciding spikes in both channels (12). Thus cross-correlation (anti-correlation) will be detected as a sensitive indication of binding, and made possible with labeling of only one binding partner. An additional strength of this analysis lies in that particles/biomolecules not carrying any ligands are estimated by iFCS, and that independently but in the same measurement, ligand-carrying particles/biomolecules are estimated by iFCCS and standard FCS. This allows direct estimation of the degree of fluorescence labeling of proteins, or more generally, direct estimation of the fraction of particles or biomolecules that carry a fluorescently labeled ligand (12).

## 5. GENERAL CONSIDERATIONS AND DISCUSSION

To date iFCS-measurements have been carried out using fluorescent dye molecules as medium (10, 12). It is important to avoid adsorption of medium-molecules to the analyzed particles, since this potentially can reduce the depth of the negative spikes caused by transiting particles, or even result in positive spikes. In analyses of negatively

charged carboxylated polystyrene microspheres, alexa 488 carboxylic acid has been used as medium (maximum negative net charge -3) (10, 12). Also for analysis of proteins the charge of the medium-molecules should be the same as that of the proteins, to avoid adsorption. For this reason, the pH of the buffer should if possible be adjusted so that the protein either has a net positive or a net negative charge, and medium-molecules with the same sign of net charge should be chosen. Precautions should be taken to avoid that the adjusted pH has undesirable effects on the properties of the studied protein. We have so far used either alexa 488 carboxylic acid (10, 12) or alexa 647, which both have a maximum negative net charge of -3.

Often the reduction in signal caused by transiting particles is difficult to observe in the intensity trace. Uncertainty may then arise whether an obtained ACF is the result of true iFCS, or the result of medium molecules adsorbed to the analyzed particles; the latter case could result in standard FCS of “labeled” particles. The uncertainty can be removed if a fluorescently labeled, but otherwise identical, version of the analyzed particles is available. If measuring iFCCS on the labeled particles results in anti-correlation, it proves that the labeled particles cause negative spikes in the medium-trace (12). If the surface properties of the labeled and unlabeled particles are identical, it is then reasonable to assume that also the unlabeled particles generate negative spikes.

If no fluorescent analogue of the analyzed particles is available, an alternative test is to reduce the concentration of fluorescent medium-molecules, and keep the excitation power constant. If the ACF is the result of dye-molecules adsorbed onto the particles, the quality of the ACF will stay constant as the dye-concentration is

## Inverse-FCS: more information and less labeling

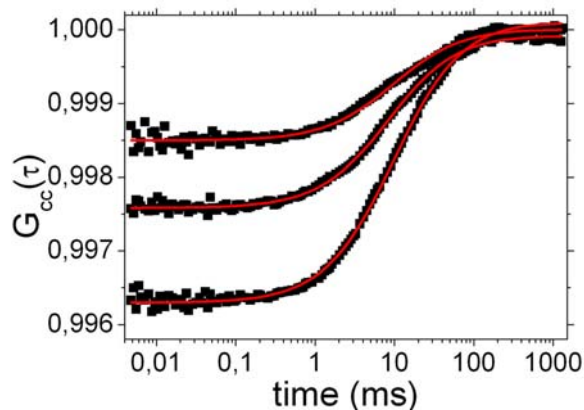


**Figure 4.** iFCCS curves from measurement on 540/560 fluospheres of 200 nm diameter in a buffer (20 mM Tris-HCl, 75 mM KCl, 0.025 percent Triton X-100, pH 8.6) containing 100 micro M alexa 488. The curves display anti-correlation because negative spikes in the medium-signal (green channel) coincide with positive spikes from the fluospheres (red channel). Starting from the lowest curve, measurements were performed on samples diluted to 2.5, 1.25 and 0.62 nM respectively. Due to the presence of cross-talk, the amplitude is dependent on particle concentration (eq. 5). Curves were fitted to a model containing one diffusion component only, resulting in a diffusion time  $\tau_D$  of 10 ms. Measurement time was 120 s.

reduced. However if the ACF is the result of iFCS, then the reduction in concentration (and count rate) will eventually make the negative spikes drown in the noise of the medium-signal, making the ACF noisier (10).

How small particles that can be analyzed by iFCS is determined by the ratio between  $V_q$  and the noise in the medium-signal, or rather between the relative noise in the medium-signal (noise/signal) and  $V_q$ . There are two main sources of noise; that from fluctuations in the number of medium-molecules in the detection volume (molecular noise), and that from fluctuations in the number of detected photons per time bin (photon noise) (10). When measurements are performed on a standard FCS-microscope equipped with APD-detectors and a diffraction-limited detection volume (about 0.3 fl), the photon noise will likely be the dominating source of noise (10). If, as an example, 500 micro M of dyes is used as medium, the average number of dye-molecules in the detection volume is 90 000, assuming a  $V_{dv}$  of 0.3 fl. Hence the average number of dye-molecules that contribute to the signal collected during one time-bin will be  $3 \cdot 10^6$  (given a bin time of 1 ms and a diffusion time  $\tau_D$  of the dye-molecules of 30 micro s) (10). The molecular noise is poisson-distributed, wherefore the standard deviation equals the square root of the mean. Accordingly, the relative molecular noise (noise/signal) equals approximately  $6 \cdot 10^{-4}$  in this example. The relative photon noise however, assuming  $7 \cdot 10^3$  photons per bin (given 7 MHz count rate and 1 ms bin time), is 0.012 in this example, about 20 times larger than the molecular noise, and thus dominates completely.

If measurements are performed in reduced detection volumes, which for example can be generated in so called zero-mode wave guides (15), the molecular noise may suddenly become important. In a detection volume of about  $10^{-19}$  liter, and using a dye concentration as high as 1 mM,  $N$  is only 60 which clearly will generate larger molecular noise. If APD-detectors are used, the photon noise will however remain approximately the same as in the example above using a diffraction-limited detection volume, because count rates of the same order can be generated and detected.

When measurements are performed on particles that are too large to be considered point-like, care has to be taken for two reasons. Firstly, when the particles radius exceeds about 20 percent of the beam radius  $\omega_0$ , the diffusion time increases more than linearly with particles radius (10, 16, 17). This explains why the measured diffusion time of the particles in Figure 3b more than doubles when the particle radius is increased by a factor of two. Thus, if the particle-size is derived from the estimated diffusion time, the size will be over-estimated unless this effect is considered (10). Secondly, if particles of sizes  $V_{part}$  that approach or even exceed the size of the detection volume  $V_{dv}$  are measured, the reduction in the medium-signal will not be given by  $V_q$ . As an example, if  $V_{part}$  equals  $V_{dv}$ , a transiting particle will only displace a fraction of the medium from the detection volume due to the different shapes of the particle and the detection volume (10).

## 6. PERSPECTIVE

iFCS and iFCCS will most likely allow analysis of considerably smaller particles and even protein molecules, by measuring in reduced detection volumes. Presently two approaches exist by which considerably reduced detection volumes can be generated, which also allow FCS-measurements: STED-microscopy (18) and measurement in so called zero-mode wave guides (ZMW) (15). With STED-microscopy the  $1/e^2$ -radius  $\omega_0$  can be reduced about 8-fold (19), however restricting the z-dimension of the STED-FCS detection volume is difficult. Although demonstrated also for solution measurements in 3-D (20), STED-FCS is preferentially of benefit for two-dimensional diffusion-studies, e.g. on cell surfaces (19). Thus, for 3-D measurements in solution, ZMWs will likely be the better choice for iFCS and iFCCS. In ZMWs, detection volumes smaller than 50 nm in all three dimensions (15) can be generated, with total volumes 1000 – 10 000 times smaller than diffraction-limited detection volumes.

Measuring iFCS and iFCCS in reduced detection volumes is one way of enabling analysis of smaller particles, since it increases  $V_q$ . An alternative is to reduce the noise in the medium-signal, since the ability to analyse smaller particles is determined by the ratio between  $V_q$  and the noise in the medium-signal. As discussed above, when measurements are performed in diffraction-limited detection volumes, using medium-concentrations of 100 micro M or above, the noise in the medium-signal will be

## Inverse-FCS: more information and less labeling

dominated by photon-noise (10). The relative noise can thus be reduced by detecting higher count rates, since the noise/signal ratio equals  $n^{1/2}/n$  which equals  $1/n^{1/2}$ , where  $n$  is the number of detected photons per time-bin. In standard FCS-instruments, either avalanche photo-diodes (APDs) or photo-multiplier tubes (PMTs) in single photon-counting mode are used, both limited to detecting count rates of about 20 – 30 MHz. Low excitation powers have therefore been used in order not to damage the detectors (10). By instead using PMTs running in current-mode, or simple photo-diodes, both capable of detecting more than  $10^{13}$  Hz (21), the detected count rates will no longer be limited by the detectors. Instead the limit will be set by the total signal that can be generated from the medium. This limit is in turn set by the maximum dye concentration that can be used without causing self-quenching (about 1 mM), combined with the maximum CPM-value (detected counts per molecule per second) obtainable. Even without trying to maximize the total count rate, we have obtained more than 1 GHz using 500 micro M of alexa 488 in a detection volume of 0.3 fl. This should enable analysis of particles of 40 nm diameter even in a diffraction-limited detection volume, which can be compared with about 100 nm diameter using APDs at count rates of 5-7 MHz in a diffraction limited detection volume (10).

A very interesting possibility is to apply iFCS/iFCCS to 2-D diffusion measurements on cell surfaces, by specifically labeling the lipids of the cell surface, and analyze the diffusion of trans-membrane proteins. Diffusion coefficients of trans-membrane proteins are often estimated in the attempt to detect dimerization or oligomerization, but the weak effect of protein size on the diffusion coefficient makes such analyses difficult. iFCS/iFCCS would be more sensitive, and able to directly measure the area of the proteins in the plane of the cell surface (12). Moreover, 2-D-measurements have an advantage since a larger fraction of the signal is displaced in 2-D as a protein enters the detection area, compared to the situation in a measurement of 3-D-diffusion. We estimate that if detectors that allow high count rates are used, a diffraction-limited detection volume should be sufficient for iFCS/iFCCS analyses for trans-membrane proteins of 5 nm diameter and larger. For iFCS/iFCCS-analysis of 2-D-diffusion of objects with diameter below 5 nm, STED-FCS should be possible to apply (19).

Fluorescent dye molecules may prove to be the best choice for signal-generating medium molecules also in future versions of iFCS. However, read-outs other than fluorescence are potentially interesting, and one alternative is to use molecules that generate raman scattering as signal (22, 23). If a higher total signal can be generated from such scatterers, a lower relative photon noise will allow smaller particles to be analyzed. In addition, strong raman scatterers can be small molecules, which may allow concentrations of more than 1 M of scattering-molecules to be used, considerably higher than what is possible for organic dye-molecules. This would reduce also the

molecular noise, which may be important especially when reduced detection volumes are used.

In iFCS, the amplitude of the ACF is determined by two parameters: the volume and the concentration of the analyzed particles (10). Therefore information about the volume of the particles cannot be deduced immediately from an iFCS-curve, as is the case in iFCCS (12). However, by using photon-counting statistics, such as PCH (24) or FIDA (25), it should be possible to determine the depth of the negative spikes, which will enable the volume of the analyzed particles to be estimated. The suitability of applying PCH or FIDA can be understood from the strong impact of the particle-size on intensity traces (compare with eq. 6). Thus independent estimates of particle volume and particle mobility will be obtained from a single measurement, and comparison between the two should give information about the shape of the particle.

In conclusion, almost 40 years after the first published realization of FCS, the methodology of FCS and related methods is still in very active development. Recently, as a part of this development iFCS was introduced as a new version of FCS, with several features likely to make it a versatile complement to standard FCS. In this review we have discussed present and also future possibilities of iFCS and iFCCS, and we look forward to the next few years as these techniques will be further improved for analysis of proteins and other biomolecules.

## 7. ACKNOWLEDGEMENTS

We are grateful for valuable discussions with Dr. Per Thyberg and Dr. Tor Sanden. We also want to acknowledge financial support from the Knut and Alice Wallenberg Foundation.

## 8. REFERENCES

1. D. Magde, E. Elson and W. W. Webb: Thermodynamic Fluctuations in a Reacting System - Measurement by Fluorescence Correlation Spectroscopy. *Phys Rev Lett* 29, 705-708 (1972)
2. E. L. Elson and D. Magde: Fluorescence correlation spectroscopy. I. Conceptual basis and theory. *Biopolymers* 13, 1-27 (1974)
3. R. Rigler, Ü. Mets, J. Widengren and P. Kask: Fluorescence Correlation Spectroscopy with High Count Rate and Low Background - Analysis of Translational Diffusion. *Eur Biophys J Biophys* 22, 169-175 (1993)
4. K. Bacia, S. A. Kim and P. Schwill: Fluorescence cross-correlation spectroscopy in living cells. *Nat Methods* 3, 83-89 (2006)
5. C. Eggeling, L. Brand, D. Ullmann and S. Jager: Highly sensitive fluorescence detection technology currently available for HTS. *Drug Discov Today* 8, 632-641 (2003)

## Inverse-FCS: more information and less labeling

6. M. Brändén, T. Sandén, P. Brzezinski and J. Widengren: Localized proton microcircuits at the biological membrane-water interface. *P Natl Acad Sci USA* 103, 19766-19770 (2006)
7. K. Palo, Ü. Mets, S. Jager, P. Kask and K. Gall: Fluorescence intensity multiple distributions analysis: Concurrent determination of diffusion times and molecular brightness. *Biophys J* 79, 2858-2866 (2000)
8. P. Kask, K. Palo, N. Fay, L. Brand, Ü. Mets, D. Ullmann, J. Jungmann, J. Pschorr and K. Gall: Two-dimensional fluorescence intensity distribution analysis: Theory and applications. *Biophys J* 78, 1703-1713 (2000)
9. S. Wennmalm and S. M. Simon: Studying individual events in biology. *Annu Rev Biochem* 76, 419-446 (2007)
10. S. Wennmalm, P. Thyberg, L. Xu and J. Widengren: Inverse-Fluorescence Correlation Spectroscopy. *Anal Chem* 81, 9209-9215 (2009)
11. P. Schwille, F. J. Meyer-Almes and R. Rigler: Dual-color fluorescence cross-correlation spectroscopy for multicomponent diffusional analysis in solution. *Biophys J* 72, 1878-1886 (1997)
12. S. Wennmalm and J. Widengren: Inverse-Fluorescence Cross-Correlation Spectroscopy. *Anal Chem* 82, 5646-5651 (2010)
13. O. Krichevsky and G. Bonnet: Fluorescence correlation spectroscopy: the technique and its applications. *Rep Prog Phys* 65, 251-297 (2002)
14. D. E. Koppel: Statistical accuracy in fluorescence correlation spectroscopy. *Phys Rev A* 10, 1938-1945 (1974)
15. M. Foquet, K. T. Samiee, X. X. Kong, B. P. Chauduri, P. M. Lundquist, S. W. Turner, J. Freudenthal and D. B. Roitman: Improved fabrication of zero-mode waveguides for single-molecule detection. *J Appl Phys* 103, 034301 (2008)
16. B. Wu, Y. Chen and J. D. Müller: Fluorescence correlation spectroscopy of finite-sized particles. *Biophys J* 94, 2800-2808 (2008)
17. K. Starchev, J. W. Zhang and J. Buffle: Applications of fluorescence correlation spectroscopy - Particle size effect. *J Colloid Interf Sci* 203, 189-196 (1998)
18. S. W. Hell: Toward fluorescence nanoscopy. *Nat Biotechnol* 21, 1347-1355 (2003)
19. C. Eggeling, C. Ringemann, R. Medda, G. Schwarzmann, K. Sandhoff, S. Polyakova, V. N. Belov, B. Hein, C. von Middendorff, A. Schönle, and S. W. Hell: Direct observation of the nanoscale dynamics of membrane lipids in a living cell. *Nature* 457, 1159-1162 (2009)
20. L. Kastrup, H. Blom, C. Eggeling and S. W. Hell: Fluorescence Fluctuation Spectroscopy in Subdiffraction Focal Volumes. *Phys Rev Lett* 94, 178104-4 (2005)
21. Hamamatsu: data sheet for PMT H6779, [www.hamamatsu.com](http://www.hamamatsu.com) (2010).
22. B. L. Li and A. B. Myers: Absolute Raman Cross-Sections for Cyclohexane, Acetonitrile, and Water in the Far-Ultraviolet Region. *J Phys Chem* 94, 4051-4054 (1990)
23. A. B. Myers, R. A. Mathies, D. J. Tannor and E. J. Heller: Excited-State Geometry Changes from Pre-Resonance Raman Intensities - Isoprene and Hexatriene. *J Chem Phys* 77, 3857-3866 (1982)
24. Y. Chen, J. D. Müller, P. T. C. So and E. Gratton: The photon counting histogram in fluorescence fluctuation spectroscopy. *Biophys J* 77, 553-567 (1999)
25. P. Kask, K. Palo, D. Ullmann and K. Gall: Fluorescence-intensity distribution analysis and its application in biomolecular detection technology. *P Natl Acad Sci USA* 96, 13756-13761 (1999)

**Key Words:** Inverse-Fluorescence Correlation Spectroscopy, inverse-Fluorescence Cross-Correlation Spectroscopy, Fluorescence Correlation Spectroscopy, Label-Free, Detection Volume, Particle-Sizing, High-Throughput Screening, Diffusion-Coefficient, Particle Shape, Review

**Send correspondence to:** Stefan Wennmalm, Department of Applied Physics, Experimental Biomolecular Biophysics, Royal Institute of Technology, 106 91 Stockholm, Sweden, Tel: 46-8-55378747, +46-8-55378216, E-mail: [stewen@kth.se](mailto:stewen@kth.se)

<http://www.bioscience.org/current/volS3.htm>